Optimization of surface-mount-device light-emitting diode packaging: investigation of effects of component optical properties on light extraction efficiency

Tomoaki Kashiwao,[a,b,*] Mayu Hiura,[a] Yee Yan Lim,[b] Alireza Bahadori,[b] Kenji Ikeda,[c] and Mikio Deguchi[a]
[a]National Institute of Technology, Niihama College, Department of Electronics and Control Engineering, 7-1 Yagumo-cho, Niihama, Ehime 792-8580, Japan
[b]Southern Cross University, School of Environment, Science and Engineering, P.O. Box 157, Lismore, New South Wales 2480, Australia
[c]Tokushima University, Graduate School of Institute of Technology and Science, 2-1 Minamijosanjima-cho, Tokushima 770-8506, Japan

Abstract. An investigation of the effects of the optical properties of surface-mount-device (SMD) light-emitting diode (LED) (side-view and top-view LEDs) packaging (PKG) components on the light extraction efficiency η_{PKG} using ray-tracing simulations is presented. In particular, it is found that the optical properties of the PKG resin and the lead-frame (L/F) silver-plating significantly affect η_{PKG}. Thus, the effects of the surface reflection methods of these components are investigated in order to optimize the optical design of the LED PKG. It is shown that there exists peak extraction efficiency for each PKG, and the cavity angle formed by the cavity wall is important to the optical design. In addition, the effect of phosphor present in the mold resin is examined using a Mie scattering simulation. Finally, an SMD LED PKG optical design method is proposed on the basis of the simulation results. [DOI: 10.1117/1.OE.55.2.025101]

Keywords: light-emitting diodes; surface-mount-device packaging; optical design; ray-tracing simulation.

Paper 151252 received Sep. 10, 2015; accepted for publication Dec. 28, 2015; published online Feb. 2, 2016.

1 Introduction

White surface-mount-device (SMD) light-emitting diodes (LEDs), which are composed of a combination of a blue LED chip and phosphor, are being used for various electronic instruments, and many LED manufacturers and researchers are engaging in intensive competition to further enhance white SMD LED performance.[1–3] Of course, improvement of the LED chip output is an important factor in the further development of all LEDs. In addition, however, improvement of the LED packaging (PKG) light extraction efficiency η_{PKG} is also important.[4–7] The PKG performance is primarily determined by the structure[8] and optical properties of the PKG components. The optical properties of PKG components are particularly important parameters as regards LED product performance, because an electric input loss of more than 10% is caused by the PKG.[4] In the case of white LEDs, the PKG is composed of various component materials, primarily PKG resin (injection molding resin), mold resin (silicone or epoxy)[9–11] containing a phosphor[12–16] and a diffuser material, a lead frame (L/F),[17,18] die-bonding paste,[19,20] and bonding wire.[21–23] Each component has been investigated intensively with regard to its performance in each area of the device. Further, ray-tracing simulations based on the Monte-Carlo method have been used for optical design in the early phase of LED product development.[24–27] This approach plays an important role in terms of both cost and time reduction. Note that the production of an LED PKG prototype has a high cost and is time consuming, because a die is required.

*Address all correspondence to: Tomoaki Kashiwao, E-mail: kashiwao@ect.niihama-nct.ac.jp

In previous studies, we investigated the effect of the optical properties of the components of an SMD LED on the device η_{PKG} using ray-tracing simulations.[28,29] In this study, we focus on the optical properties of PKG resin and L/F silver-plating. The optical properties of these materials have a significant effect on the η_{PKG} of LED PKG. Here, the effects of the PKG resin and L/F silver-plating reflection methods in particular are investigated. Side-view (SV) LEDs, which are used for liquid-crystal display (LCD) backlights, and top-view (TV) LEDs, which are used for general purposes such as LED illumination, are considered in this study. Note that the SV PKG cavity is narrower and the light reflection frequency is higher than those of a general LED PKG. On the other hand, the TV PKG cavity wall functions as a light reflector. Therefore, the reflection methods dependent on the component surface conditions are important to the LED PKG design. In addition, the phosphor in the mold resin has a significant effect on the η_{PKG}.[30–34] In this study, we investigate the relationship between the component reflection methods (the PKG resin and the L/F silver-plating) and the η_{PKG} of the LED PKG using ray-tracing simulations in order to confirm the possibility of optimizing this device. Moreover, a simulation considering the phosphor contained in the mold resin is performed in order to investigate the effect of this substance on the η_{PKG}. Finally, important points regarding the SMD PKG optical design method are presented, which are based on the simulation results.

In Sec. 2, the ray-tracing simulation is explained and the definition of the η_{PKG} examined in this study is presented. In Sec. 3, the simulation conditions are explained and the simulation results are shown and discussed. Finally, Sec. 4 concludes the paper.

2 Ray-Tracing Simulation

In this study, the LightTools 8.0.0, 8.1.0, and 8.2.0 (Synopsys, Inc.) packages are used for the ray-tracing simulations (Fig. 1). Numerous rays are emitted from the top surface of an LED chip in the top and bottom directions according to the simulated distributions. The rays undergo repeated reflection and refraction several times in the LED PKG cavity, and the intensities decrease according to the reflection surface reflectance (Fresnel loss is ignored for ray refraction in this study). Finally, the rays are emitted from the LED PKG. Thus, the optical properties of the PKG components significantly affect the PKG performance.

2.1 *Light Extraction Efficiency*

η_{PKG} is used as an index to verify the LED PKG performance and is defined as

$$\eta_{\mathrm{PKG}} = \frac{\sum_n I_{Pn}}{\sum_n I_{Cn}}, \tag{1}$$

where I_{Pn} and I_{Cn} are the relative intensities emitted from the PKG and LED chip, respectively, $n = 1, \ldots, N$ is the ray number, and N is the number of rays. (The η_{PKG} calculation is based on the total radiant flux, measured in Watt.) Thus, the PKG η_{PKG} means the ratio of the total relative intensity that is not absorbed by the LED PKG. As noted above, the η_{PKG} values of SV and TV PKG, such as those shown in Fig. 2, are investigated in this study.

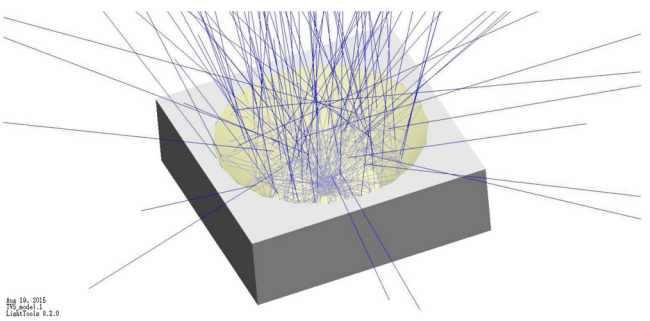

Fig. 1 LightTools ray-tracing simulation image.

2.2 *Reflection Methods*

Mirror (specular), Gaussian, and Lambertian reflections are the reflection methods operating on the surfaces of the PKG resin and L/F silver-plating of each PKG. The Gaussian reflection angle is determined according to the Gaussian function, with the mean being determined by considering the angle of the mirror reflection and the standard deviation σ, which represents the degree of scattering (mirror reflection corresponds to $\sigma = 0$ deg). Lambertian reflection corresponds to complete scattering. Gaussian reflection at $\sigma = 0$ to 30 deg in 1-deg increments and Lambertian reflection are the reflection methods considered in this study. The η_{PKG} of each PKG is calculated for 1024 combinations of the PKG resin and L/F reflection methods in the simulations.

When rays are reflected from the cavity wall surface and L/F, the relative intensity can be expressed as

$$I_n = \rho I_n, \tag{2}$$

where I_n is the relative intensity before emission from the PKG and ρ is the reflectance of the reflection surface. Thus, higher reflectance is both preferable and important in each case. In addition, the greater the number of repeat reflections in the cavity, the smaller the eventual η_{PKG}. Consequently, the PKG optical design should aim to reduce reflection repetition in the cavity.

In the ray-tracing simulation, actual scattering on the surface of the PKG resin and the L/F silver-plating can be modeled as Gaussian reflection for $\sigma = 30$ deg and over and $\sigma \approx 15$ deg, respectively, according to comparisons between the simulation and actual experimental results. However, the surface conditions are affected by the surface processing methods and materials. For example, the PKG resin reflection method and reflectance are affected by the surface processing conditions of the resin die, its materials (e.g., polyamide is generally used), and its components (e.g., the percentage of titanium oxide). In addition, the silver-plating reflection method is close to mirror reflection and its reflectance is higher than that of general materials; however, these characteristics are significantly affected by the electroplating method. Therefore, the choice of PKG components significantly affects the optical performance of the LED PKG.

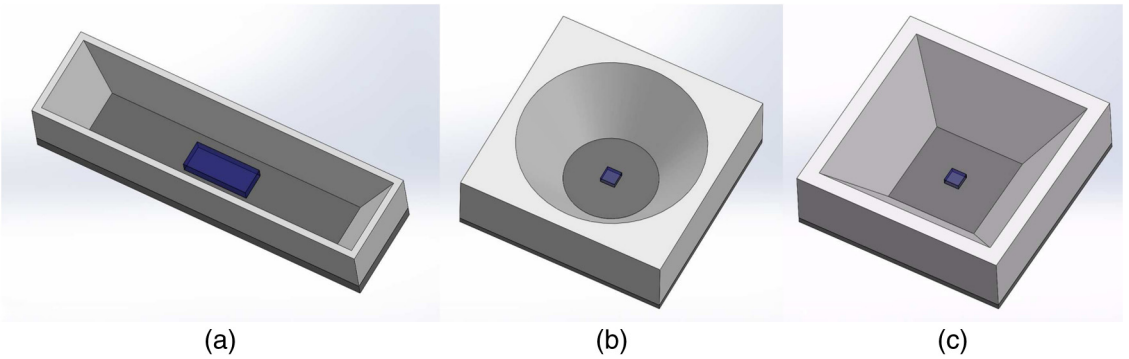

Fig. 2 PKG without mold resin (a) SV PKG, (b) TV PKG with round cavity, and (c) TV PKG with square cavity.

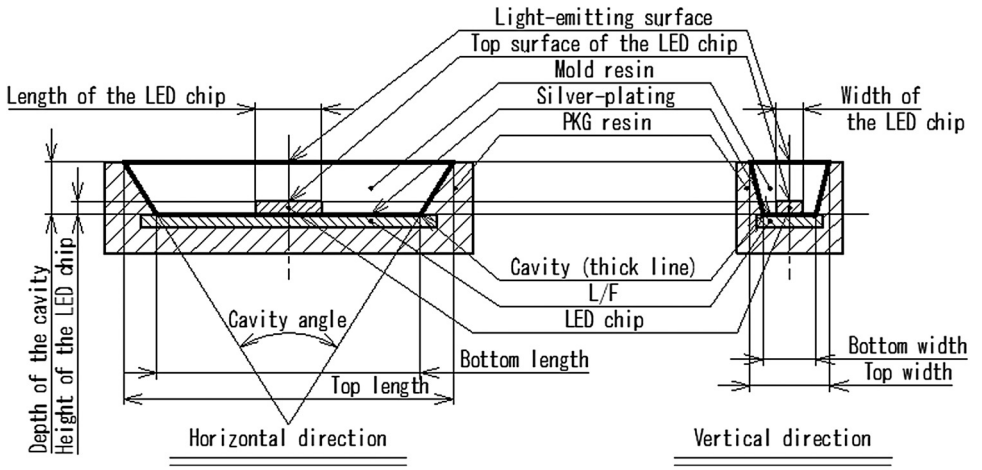

Fig. 3 Dimensions of SMD LED PKG components.

3 Simulation

3.1 *Simulation Conditions*

Figure 3 shows the names and dimensions of the LED PKG components, whereas Tables 1 and 2 show the simulation parameters. The SV PKG models are of three different sizes. In addition, TV PKG models with three different round-cavity bottom diameters and three different square-cavity side bottom lengths are investigated. Both PKG types are already internationally widespread. As noted above, SV PKG is used for LCD backlights in electrical appliances, such as smart phones. Thus, the SV LED has a thin PKG (<1.0 mm) and a narrow cavity (Fig. 4). On the other hand, the TV PKG is used for general LEDs with a high output. Both types are still undergoing development and are being enhanced rapidly and intensively. Round- and square-shaped cavities are generally used. In this study, the optimal shape for TV PKG is confirmed.

Table 3 shows the common simulation conditions. The optical properties were obtained from the widely used values for these materials. The LED chip was modeled as a cuboid sapphire with a refractive index of 1.78. The refractive index of sapphire depends on the wavelength of the incident light, and it is ~1.78 for the wavelength of the blue light emitted from the LED chip. In practice, the structure of the LED chip

Table 1 SV PKG dimensions.

		SV1	SV2	SV3
Horizontal direction	Top length (mm)	0.4	0.6	0.8
	Bottom length (mm)	0.3	0.4	0.5
Vertical direction	Top width (mm)	2.0	2.5	3.0
	Bottom width (mm)	1.5	2.0	2.5
Cavity depth (mm)		0.35	0.4	0.45
LED chip dimensions (mm)		L 0.5 × W 0.2 × H 0.1		

Table 2 TV PKG dimensions.

	TV4	TV5	TV6	TV7	TV8	TV9
Cavity shape	Round			Square		
Top length (mm)	3.0 (diameter)			3.0 (side length)		
Bottom length (mm)	1.0	1.5	2.0	1.0	1.5	2.0
Cavity depth (mm)	1.0	1.0	1.0	1.0	1.0	1.0
LED chip dimensions (mm)	L 0.25 × W 0.25 × H 0.1					

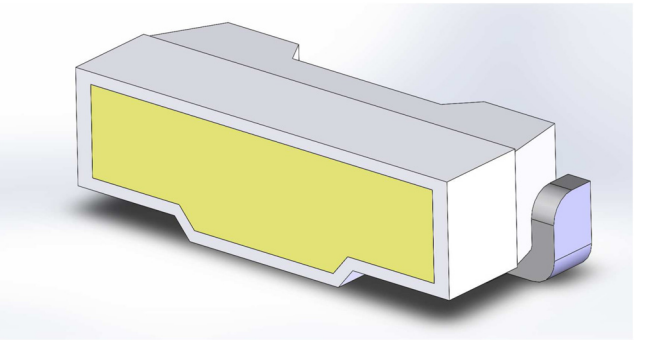

Fig. 4 SV LED packaging.

Table 3 Common simulation parameters.

Parameter	Value
PKG resin reflectance	0.9
L/F silver-plating reflectance	0.95
Mold resin refractive index	1.43
LED chip refractive index	1.78
LED chip light emission type	Lambertian
Ray number	2,000,000

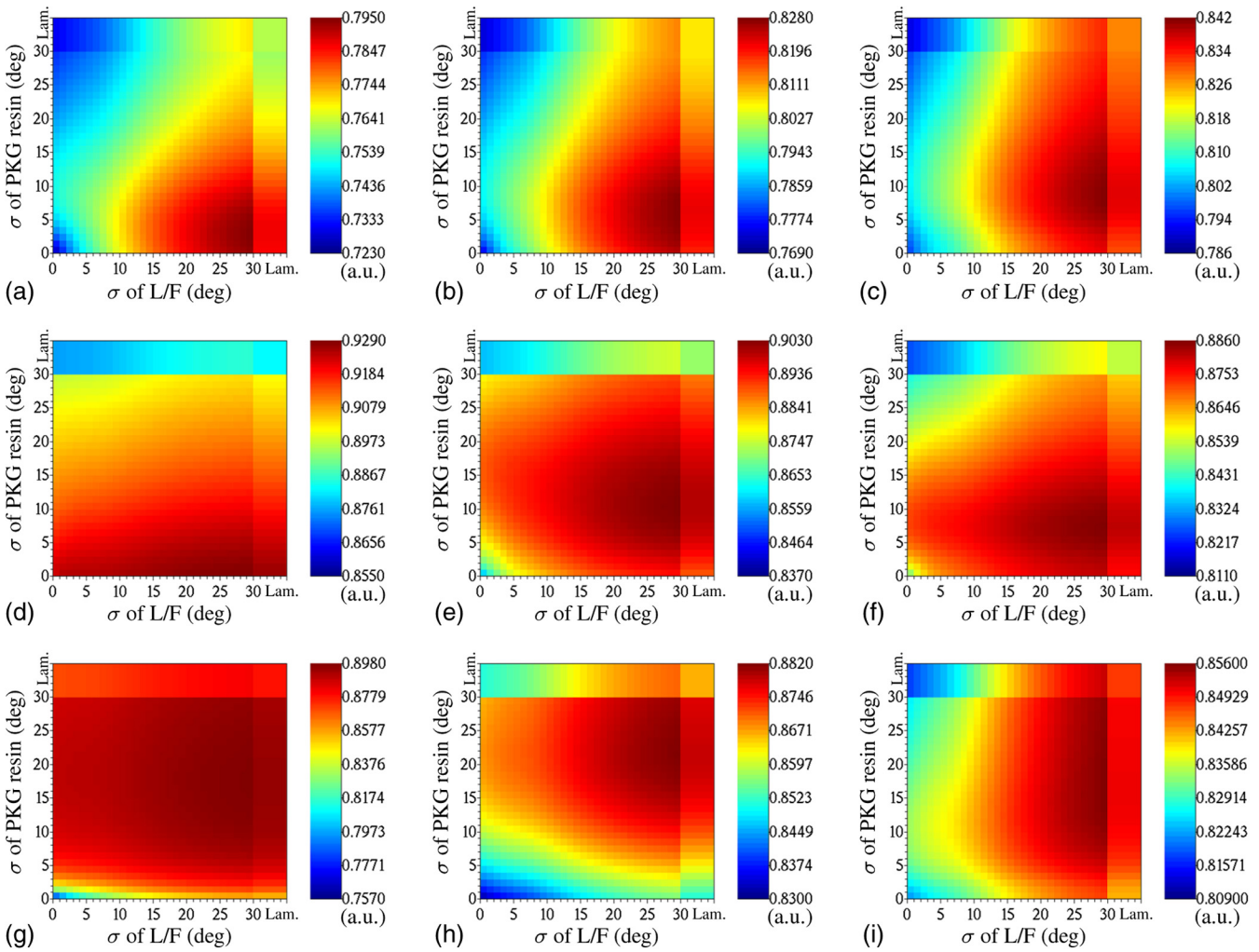

Fig. 5 η_{PKG} distributions for various PKG and L/F combinations (arbitrary unit: a.u.). The vertical and horizontal axes are the σ of the PKG resin and L/F silver-plating, respectively: (a) SV1, (b) SV2, (c) SV3, (d) TV4, (e) TV5, (f) TV6, (g) TV7, (h) TV8, and (i) TV9. $\sigma > 30$ deg corresponds to Lambertian reflection.

Table 4 Maximum and minimum η_{PKG} values of each PKG.

PKG	Maximum value			Minimum value		
	η_{PKG} (a.u.)	Resin: σ (deg)	L/F:σ (deg)	η_{PKG} (a.u.)	Resin:σ (deg)	L/F: σ (deg)
SV1	0.795	3	30	0.723	0	0
SV2	0.828	6	30	0.769	Lambertian	0
SV3	0.842	8	30	0.786	Lambertian	0
TV4	0.929	0	30	0.855	Lambertian	0
TV5	0.903	10	30	0.837	Lambertian	0
TV6	0.886	7	30	0.811	Lambertian	0
TV7	0.898	18	30	0.757	0	0
TV8	0.882	22	30	0.830	0	0
TV9	0.856	15	30	0.809	Lambertian	0

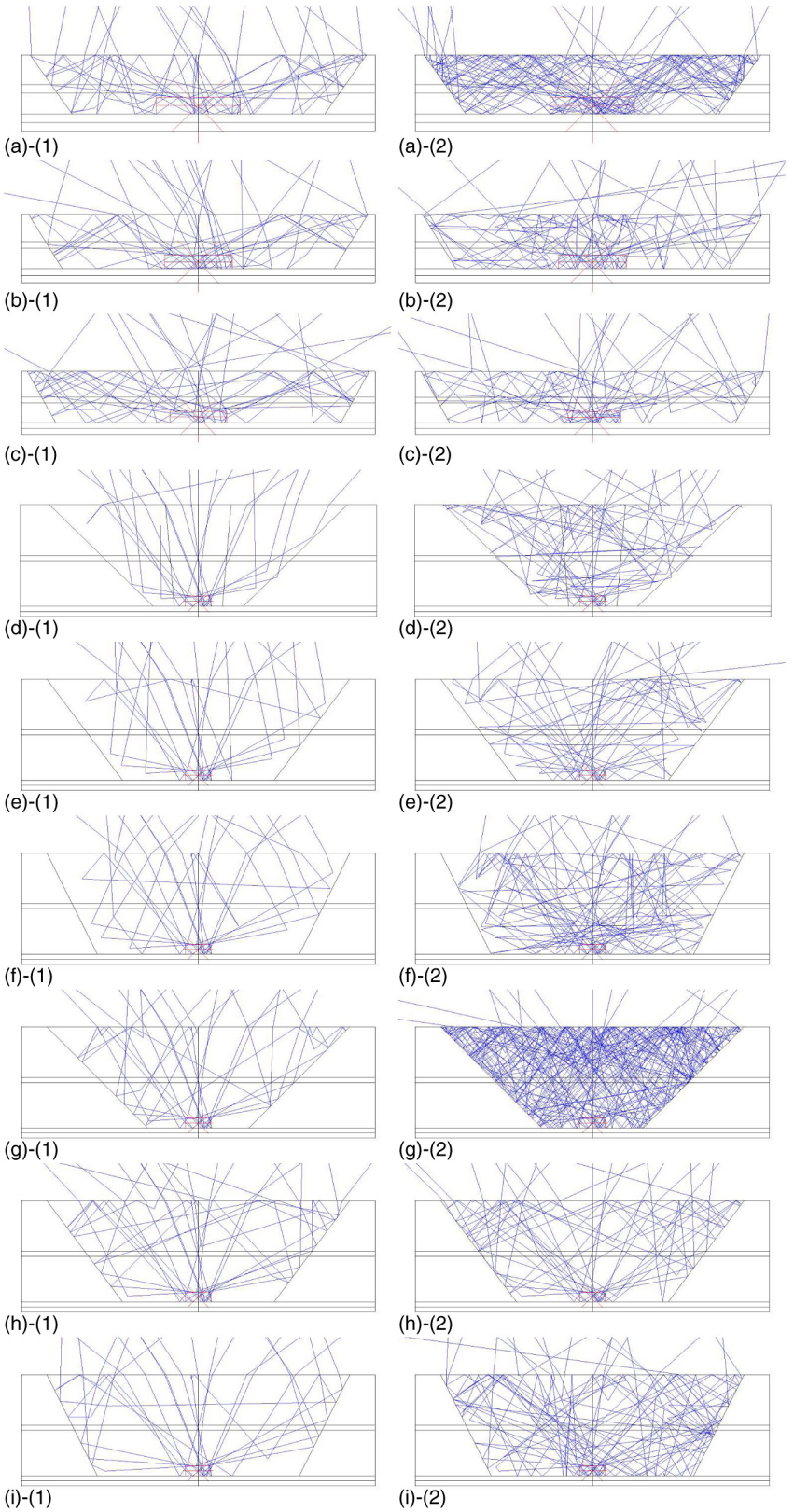

Fig. 6 Ray-tracing simulation (20 rays): PKG resin and L/F combinations corresponding to maximum and minimum η_{PKG} values for each PKG. (a) SV1, (b) SV2, (c) SV3, (d) TV4, (e) TV5, (f) TV6, (g) TV7, (h) TV8, and (i) TV9. (1) and (2) represent maximum and minimum η_{PKG} values, respectively.

significantly affects the device η_{PKG} because of the absorption in its P-GaN, InGan active, N-GaN, and electrode layers. Moreover, there exist several types of blue LED chips, namely, a horizontal, vertical (thin GaN chip), and flip chip,[35] and the emission efficiencies of these LED chips differ from each other. However, in this study, the ray emission is set as a simple Lambertian distribution from the top surface of the LED chip in the upward and downward directions, ignoring the absorption and transmittance of the sapphire. This is done to facilitate easy extraction of the effect of the PKG resin and L/F silver-plating surface conditions only on the η_{PKG}. In addition, the refractive index of the mold resin is set to 1.43 in the simulation, because silicone may have refractive index values of roughly 1.4 to 1.55; therefore, this value is not very well defined. If the mold resin refractive index is increased, the critical angle is decreased, and the rays are reflected from the light-emitting surface into the PKG cavity as a result of the total reflection on the interface between the mold resin and the air. Hence, η_{PKG} is decreased. Generally, the refractive index of silicone is smaller than that of epoxy; therefore, silicone is chosen as the mold resin for LED PKG in which high efficiency is required. (The transmittance of the mold resin is ignored in this study.) Furthermore, the higher the reflectance of the PKG resin and the L/F silver-plating, the higher the η_{PKG} (essentially). Thus, the reflectance performance of these materials, which we wish to enhance, is dependent on their surface conditions, which are, in turn, determined by the fabrication processes. Generally, in the case of higher values, the reflectance of polyamide containing titanium oxide and the silver-plating products used for the LED PKG is roughly 90% to 95% and 95% to 97%, respectively; however, these values differ widely among manufacturers in accordance with the various types of technology employed in the fabrication processes.

3.2 *Simulation Results*

Figure 5 shows the simulation results. The η_{PKG} distributions of all the PKG exhibit mountain-shaped profiles. One peak and neighboring troughs can be observed in the distributions of each PKG (Table 4). It is preferable for the PKG resin reflection to be close to mirror reflection. The TV4 cavity angle can be considered to be of the appropriate degree, because it yields the maximum value and the highest value of all the PKG when the PKG resin reflection is mirror-like. This suggests that the cavity wall functions as a light reflector (Fig. 6). On the other hand, the SV PKG performance is dependent on the PKG size, because of the narrow vertical direction of its PKG. However, when the results for the round-cavity PKG are compared to those of the square-cavity PKG, the η_{PKG} of the round cavity is higher than that of the square cavity overall, despite the larger size of the latter. It can be observed that a number of the round-cavity reflections are smaller than those for the square-cavity case in the ray-tracing simulation of Fig. 6. In the square-cavity case, the angle of the plane surface toward the cavity center point is inconsistent, and the rays are reflected between the edges of the adjacent plane surfaces. However, this does not occur in the case of the round cavity. In addition, the extraction efficiencies of all the PKG are at maxima when the standard deviation of the L/F is at $\sigma = 30$ deg and at minima when the standard deviation of the L/F is at $\sigma = 0$ deg. Therefore, the reflection on the L/F should correspond to moderate scattering rather than mirror reflection. The total number of reflected rays in the PKG cavity decreases when the L/F surface reflection causes greater scattering, because the scattering tends to prevent total reflection on the PKG light-emitting surface. This can be recognized explicitly by comparing (1) and (2) of each PKG in Fig. 6.

Figure 7 shows graphs of the η_{PKG} and absorption ratios of the PKG resin and L/F for the conditions corresponding to maximum and minimum η_{PKG} values, respectively. The η_{PKG} is higher if the absorption ratios of the PKG resin and L/F are lower. In addition, greater ray absorption is exhibited by the PKG resin in comparison to the L/F in all the simulation results. This means that the PKG performance is more significantly affected by the PKG resin optical design than that of the L/F.

3.3 *Effect of a Phosphor*

In the case of white LEDs, the mold resin contains yellow phosphors to convert blue light emitted from the LED chip to white light. The LED emission efficiency is more

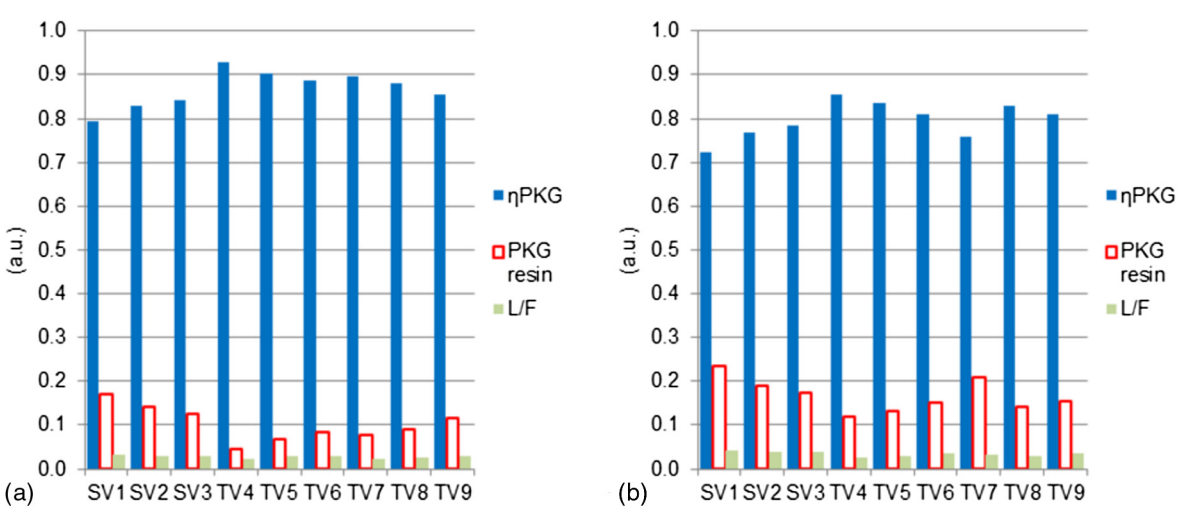

Fig. 7 η_{PKG} values and absorption ratios of PKG resin and L/F under conditions corresponding to (a) maximum and (b) minimum η_{PKG} values for each PKG.

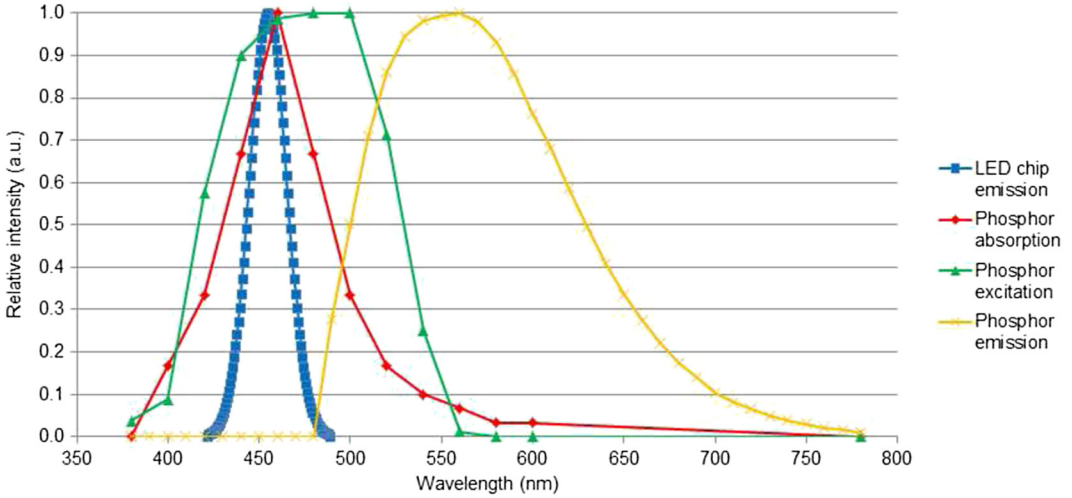

Fig. 8 LED chip emission spectrum (blue) and phosphor absorption (red), excitation (green), and emission (yellow) spectra. The emission spectrum is for all wavelengths of the excitation spectrum.

significantly affected by the internal quantum efficiencies of the phosphors than the structures and optical properties of the LED PKG components.[30–34] There exists a down-conversion loss known as the "Stokes loss," which is caused by the difference in the energy between the absorbed and emitted photons in the light wavelength conversion process.[36] In addition, it is understood that the scattering caused by the phosphor contained within the mold resin affects the

Table 5 η_{PKG} of each PKG for combinations corresponding to maximum and minimum η_{PKG} values in simulation incorporating phosphor.

		Percentage of phosphor by volume (%)					
PKG	Combination	0	1	2	3	4	5
SV1	Maximum	0.79479	0.324044	0.170071	0.093153	0.052276	0.029689
	Minimum	0.72308	0.319442	0.166891	0.090814	0.050815	0.029062
SV2	Maximum	0.82816	0.310120	0.146984	0.072563	0.036873	0.019147
	Minimum	0.76912	0.300559	0.142330	0.070215	0.035718	0.018599
SV3	Maximum	0.84231	0.286228	0.121895	0.054349	0.024984	0.011830
	Minimum	0.78577	0.279097	0.118765	0.052834	0.024405	0.011573
TV4	Maximum	0.92947	0.088049	0.012065	0.002009	0.000405	0.000137
	Minimum	0.85463	0.085842	0.011923	0.001949	0.000416	0.000127
TV5	Maximum	0.90269	0.087252	0.012029	0.002024	0.000422	0.000144
	Minimum	0.83677	0.085419	0.011923	0.001968	0.000433	0.000136
TV6	Maximum	0.88603	0.086201	0.012023	0.002041	0.000429	0.000147
	Minimum	0.81055	0.084842	0.011902	0.001983	0.000439	0.000141
TV7	Maximum	0.89815	0.087950	0.012070	0.002017	0.000413	0.000139
	Minimum	0.75738	0.086884	0.011964	0.001967	0.000423	0.000133
TV8	Maximum	0.88192	0.087351	0.012079	0.002034	0.000427	0.000147
	Minimum	0.83013	0.086476	0.011976	0.001988	0.000438	0.000141
TV9	Maximum	0.85559	0.086735	0.012064	0.002052	0.000434	0.000150
	Minimum	0.80875	0.085547	0.011981	0.001990	0.000444	0.000143

(unit: a.u.)

η_{PKG}. Thus, in this study, we investigate the effect of the phosphors using a Mie scattering simulation performed using LightTools 8.2.0, for a mold resin containing uniformly distributed phosphor particles.[36–38] In the simulation, the absorption, excitation, and emission spectrum distributions of the phosphor are set as default parameters in LightTools 8.2.0. The phosphor particle radius is set to 1000 nm as the default setting. (The phosphor particle size is roughly 1 to 30 μm, in general.) These parameters are close to the properties of yttrium aluminum garnet: cerium (YAG:Ce), which is generally used for white LEDs based on a blue LED chip (Fig. 8). [The excitation (absorption) and emission spectra of YAG:Ce have peak wavelengths at ~460 and in the range of 550 to 560 nm, respectively.] The spectrum distribution of the blue LED chip is set as a Gaussian distribution (center wavelength: 455 nm, full width at half maximum: 24 nm).[38] (A blue LED chip with a peak wavelength of 450 to 470 nm is used for white LEDs.)

The volume percentage of the phosphor in the mold resin is varied between 1% and 5% in 1% increments, and the η_{PKG} of the LED PKG for the PKG resin and L/F silver-plating combinations shown in Table 4 are verified. Table 5 shows the results of the simulation considering the phosphor. Hence, it can be observed that the higher the phosphor percentage by volume, the smaller the difference in the extraction efficiency η_{PKG} between the maximum and minimum conditions. In addition, if the phosphor percentage is increased, the absorption ratios of the PKG resin are decreased and those of the L/F are increased (Fig. 9). This is because the rays cannot reach the cavity wall (the PKG resin) as a result of the scattering caused by the phosphors (Fig. 10). Thus, the L/F reflectance becomes more important when the mold resin includes phosphors. In the case of SV PKG, the rays can reach the cavity wall because of the narrow cavity (Fig. 11). The absorption ratios of the SV1, TV4, and TV7 PKG at 1% phosphor by volume are higher than those at 0%, because the number of rays reflected in the cavity are increased by the scattering [Figs. 10(b) and 11(b)].

3.4 *Discussion*

From the simulation results, the following SMD PKG optical design procedure can be proposed:

Step 1-1: The largest possible cavity size should be designed in the case of SV PKG.

Step 1-2: A round rather than a square cavity should be chosen in the case of TV PKG, if possible.

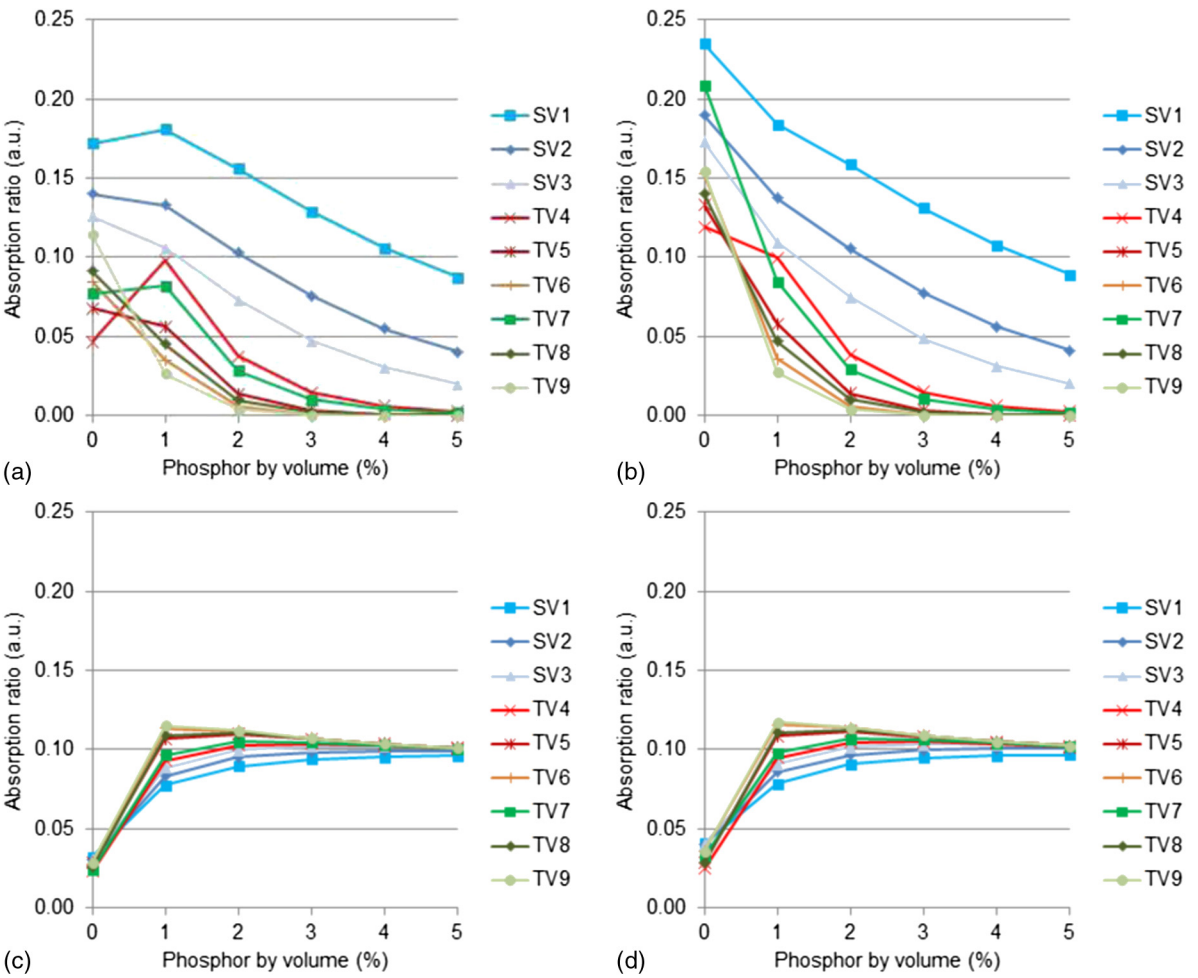

Fig. 9 Absorption ratios for phosphor-containing mold resin: PKG resin under conditions corresponding to (a) maximum and (b) minimum η_{PKG} values. L/F under conditions corresponding to (c) maximum and (d) minimum η_{PKG} values.

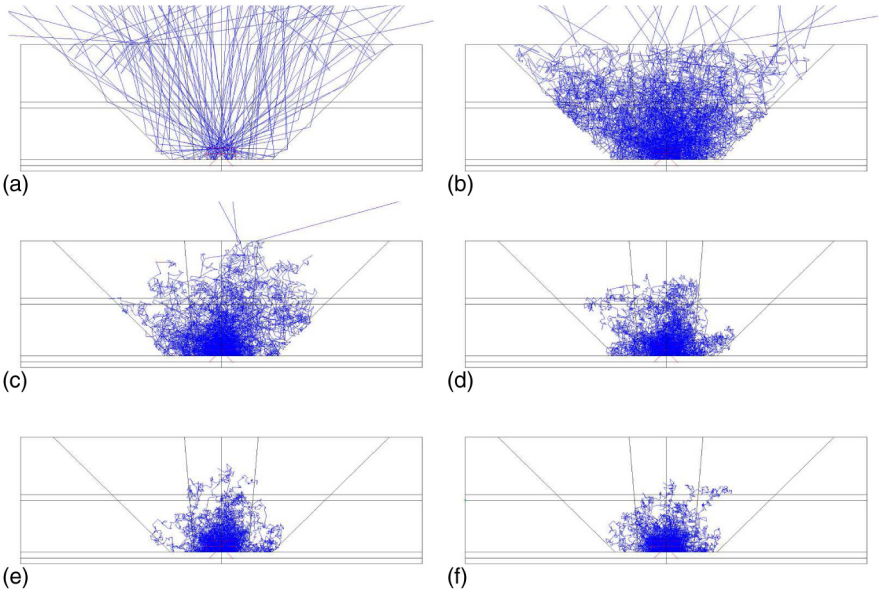

Fig. 10 Ray-tracing simulation (100 rays) of TV4 for phosphor-containing mold resin: (a) 0%, (b) 1%, (c) 2%, (d) 3%, (e) 4%, and (f) 5% phosphor by volume.

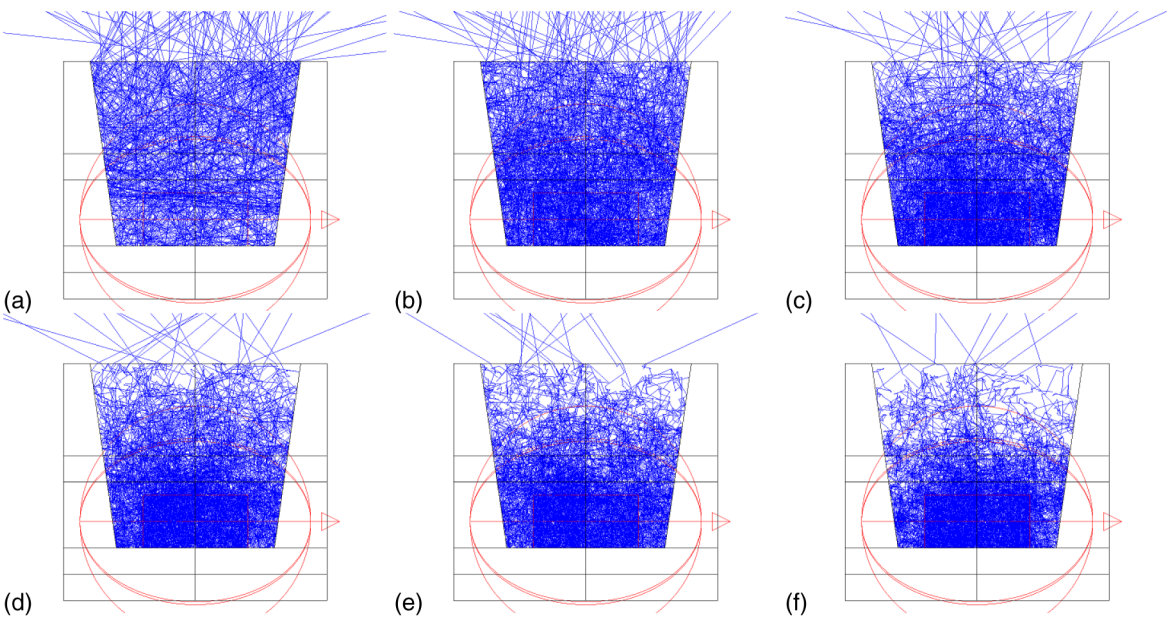

Fig. 11 Ray-tracing simulation (100 rays) of SV1 for phosphor-containing mold resin: (a) 0%, (b) 1%, (c) 2%, (d) 3%, (e) 4%, and (f) 5% phosphor by volume.

Step 2: The optimal cavity angle should be calculated using the ray-tracing simulation, considering the mirror reflection property of the PKG resin.

Step 3: It is preferable to have the PKG resin reflectance as close to mirror reflection as possible.

Designers and engineers must design LED PKG under certain restrictions in order to satisfy specific target product requirements. Thus, the cavity angle should be designed to be as close as possible to mirror reflection in Step 2 above in cases where a cavity angle corresponding exactly to mirror reflection is unrealistic. In addition, it is impossible to obtain complete mirror reflection using the examined components in reality. However, we can choose a combination of the PKG resin and L/F reflection methods that yield results as close as possible to the peak of the η_{PKG} distribution, because the distribution exhibits a mountain shape with a single peak (Fig. 5).

From the simulation results, it is preferable that the L/F silver-plating reflection exhibits proper scattering; however, the more the reflection is scattered, the lower the reflectance in actuality. Consequently, an investigation of the relationship between the silver-plating scattering profile and reflectance using physical experiments is required. In the case where the mold resin includes a high phosphor content ratio, the effect of the optical properties of the PKG resin

is reduced; however, it is still apparent for a low phosphor ratio (Fig. 9). This is especially true for the SV PKG, which has a narrow cavity. Moreover, the L/F silver-plating reflectance is more important in the presence of phosphor, because the absorption caused by the L/F is increasing.

4 Conclusion

This paper reports on an investigation of the effects of the PKG resin and L/F silver-plating surface reflection methods on the η_{PKG} values of SV and TV LED PKG using ray-tracing simulations. From the simulation results, the η_{PKG} distributions of each PKG were found to exhibit mountain-shaped profiles with a single peak, and this suggests a possibility for optimization of SMD LED PKG. In addition, a larger SV PKG cavity was shown to be preferable, because of the narrowness of the cavity in the vertical direction. Moreover, the cavity angle is important as regards TV and SV PKG design, because the cavity wall functions as the light reflector. If the maximum η_{PKG} of the TV PKG for mirror reflection can be determined, the appropriate PKG cavity angle can be obtained. In addition, a round-cavity PKG is preferable to a square-cavity device, because ray reflection occurs between the adjacent walls in the square cavity. Furthermore, the optical design of the PKG resin was shown to be more important than that of the L/F silver-plating, based on the absorption ratio results. In addition, the effect of the presence of phosphor on η_{PKG} was investigated. It was found that the importance of the PKG resin optical properties decreases, whereas that of the L/F silver-plating reflectance increases for a mold resin containing phosphors. Finally, an optical design method based on the experimental results was proposed.

In future work, we will investigate the effect of the structure and optical properties of the LED chip on the η_{PKG}. Furthermore, the simulation results and the optical properties of the components should be compared with measured results for actual LEDs and components in order to confirm the accuracy of the optical design based on the ray-tracing simulation.

Acknowledgments

This work was supported by the National Institute of Technology, Niihama College, Japan, and Southern Cross University, Australia. We are grateful to Prof. Takao Shiomomura, Prof. Koichi Suzuki, and Prof. Scott T. Smith for their support.

References

1. K. Bando et al., "Development of high-bright and pure-white LED lamps," *J. Light Visual Environ.* **22**(1), 2–5 (1998).
2. I. Niki et al., "White LEDs for solid state lighting," *Proc. SPIE* **5187**, 1 (2004).
3. Y. Narukawa et al., "Ultra-high efficiency white light emitting diodes," *Jpn. J. Appl. Phys.* **45**(10L), L1084 (2006).
4. K. Bando, "Performance of high-luminous efficacy white leds," *J. Light Visual Environ.* **35**(3), 192–196 (2011).
5. N. T. Tran and F. G. Shi, "LED package design for high optical efficiency and low viewing angle," in *Microsystems, Packaging, Assembly and Circuits Technology (IMPACT 2007). Int.*, pp. 10–13, IEEE (2007).
6. S. Liu and X. Luo, *Led Packaging for Lighting Applications: Design, Manufacturing, and Testing*, John Wiley & Sons (Asia) Pte Ltd, Singapore (2011).
7. K. H. Kim et al., "Effects of the optical absorption of a LED chip on the LED package," *Solid-State Electron.* **111**, 166–170 (2015).
8. H. Sun et al., "The model about the package structure of LED and the light intensity distribution," *Proc. SPIE* **9276**, 927610 (2014).
9. A. W. Norris, M. Bahadur, and M. Yoshitake, "Novel silicone materials for LED packaging," *Proc. SPIE* **5941**, 594115 (2005).
10. M. Bahadur et al., "Silicone materials for LED packaging," *Proc. SPIE* **6337**, 63370F (2006).
11. X. Yang et al., "Preparation and performance of high refractive index silicone resin-type materials for the packaging of light-emitting diodes," *J. Appl. Polym. Sci.* **127**(3), 1717–1724 (2013).
12. S. Fujita et al., "YAG glass-ceramic phosphor for white LED (i): background and development," *Proc. SPIE* **5941**, 594111 (2005).
13. S. Tanabe et al., "YAG glass-ceramic phosphor for white LED (ii): luminescence characteristics," *Proc. SPIE* **5941**, 594112 (2005).
14. S. Fujita, A. Sakamoto, and S. Tanabe, "Luminescence characteristics of YAG glass–ceramic phosphor for white LED," *IEEE J. Sel. Top. Quantum Electron.* **14**(5), 1387–1391 (2008).
15. S. Fujita, Y. Umayahara, and S. Tanabe, "Influence of light scattering on luminous efficacy in Ce:YAG glass-ceramic phosphor," *J. Ceram. Soc. Jpn.* **118**(1374), 128–131 (2010).
16. S. Nishiura et al., "Properties of transparent Ce:YAG ceramic phosphors for white LED," *Opt. Mater.* **33**(5), 688–691 (2011).
17. Z. Xu et al., "Reflection characteristics of displacement deposited Sn for LED lead frame," *Mater. Trans.* **53**(5), 946–950 (2012).
18. Y. Yuan, H. Wang, and J. G. Liu, "An overview of light decay failure modes in lead-frame LED packages," in *11th China Int. Forum on Solid State Lighting (SSLCHINA)*, pp. 165–169, IEEE (2014).
19. M. Kuramoto et al., "Die bonding for a nitride light-emitting diode by low-temperature sintering of micrometer size silver particles," *IEEE Trans. Compon. Packag. Technol.* **33**(4), 801–808 (2010).
20. M. Kuramoto et al., "New silver paste for die-attaching ceramic light-emitting diode packages," *IEEE Trans. Compon. Packag. Manuf. Technol.* **1**(5), 653–659 (2011).
21. B. Wu et al., "Effect of gold wire bonding process on angular correlated color temperature uniformity of white light-emitting diode," *Opt. Express* **19**(24), 24115–24121 (2011).
22. H. H. Tsai et al., "An innovative annealing-twinned Ag-Au-Pd bonding wire for IC and LED packaging," in *7th Int.Microsystems, Packaging, Assembly and Circuits Technology Conf.*, pp. 243–246, IEEE (2012).
23. J. Wu et al., "Bonding of Ag-alloy wire in LED packages," in *35th IEEE/CPMT Int. Electronic Manufacturing Technology Symp.*, pp. 1–4, IEEE (2012).
24. O. Shmatov, "Light extraction study of LED using ray tracing computer simulation," *Phys. Status Solidi (c)* **4**(5), 1629–1632 (2007).
25. N. Okada, "Optical simulation analysis for development of leading-edge electronic device," *Toshiba Rev.* **64**(5), 34–37 (2009) (in Japanese).
26. T. Kashiwao et al., "Development of a 2D optical simulator for SMD LED packaging," *J. Light Visual Environ.* **38**(0), 44–47 (2014).
27. T. Kashiwao, "A ray-tracing simulation technique for optical design of LED packaging," *Chem. Eng.* **60**(2), 101–110 (2015) (in Japanese).
28. T. Kashiwao et al., "Effect of optical properties of construction elements for light extraction efficiency of SMD LEDs," in *Proc. of SICE Annual Conf.*, pp. 1936–1940, SICE (2014).
29. M. Hiura et al., "Effect of optical properties of construction elements for light extraction efficiency in side view LED packaging," in *Proc. of Int. Symp. on Technology for Sustainability*, National Taipei University of Technology and National Institute of Technology of Japan (2014).
30. H. Luo et al., "Analysis of high-power packages for phosphor-based white-light-emitting diodes," *Appl. Phys. Lett.* **86**(24), 243505 (2005).
31. Z. Liu et al., "Optical analysis of phosphor's location for high-power light-emitting diodes," *IEEE Trans. Device Mater. Reliab.* **9**(1), 65–73 (2009).
32. N. T. Tran, J. P. You, and F. G. Shi, "Effect of phosphor particle size on luminous efficacy of phosphor-converted white LED," *J. Lightwave Technol.* **27**(22), 5145–5150 (2009).
33. C. Y. Chen et al., "High-efficiency white LED packaging with reduced phosphor concentration," *IEEE Photonics Technol. Lett.* **25**(7), 694–696 (2013).
34. C. C. Sun et al., "Packaging efficiency in phosphor-converted white LEDs and its impact to the limit of luminous efficacy," *J. Solid State Light* **1**(1), 1–17 (2014).
35. O. Shchekin et al., "High performance thin-film flip-chip InGaN-GaN light-emitting diodes," *Appl. Phys. Lett.* **89**(7), 071109 (2006).
36. M. W. Zollers et al., "Process to measure particulate down-converting phosphors and create well-correlated software models of LED performance," *Proc. SPIE* **7954**, 795414 (2011).
37. M. Zollers, "Phosphor modeling in LightTools ensuring accurate white LED models," in *LightTools White Paper*, Synopsys, Inc. (2011).
38. "Phosphor modeling in LightTools," in *Materials of LightTools Advanced Training*, Synopsys, Inc. (2012).

Tomoaki Kashiwao has been an assistant professor at the National Institute of Technology, Niihama College, Japan, since 2010 and a visiting fellow at Southern Cross University, Australia, since 2015. He received his BE, ME, and DrEng degrees from Tokushima University, Japan, in 2003, 2005, and 2009, respectively. In 2005,

he joined the Nichia Corporation as an LED packaging design engineer. His research interests include hybrid systems, LED packaging, and neural networks.

Mayu Hiura has been a student of the advanced engineering course electronic engineering program, the National Institute of Technology (NIT), Niihama College, Japan, since 2014. She received her associate degree in engineering from NIT, Niihama College, in 2014. She has studied the optical design of LED packaging.

Yee Yan Lim is currently a civil engineering lecturer in the School of Environment, Science, and Engineering, Southern Cross University, Australia. He received his bachelor's degree in civil engineering from Nanyang Technological University, Singapore, in 2004, and his PhD from the same institution in 2012. His research interest is smart-materials-based structural health monitoring and energy harvesting.

Alireza Bahadori is a lecturer and researcher with the School of Environment, Science and Engineering at Southern Cross University, Lismore, NSW, Australia. He received his PhD from Curtin University, Perth, WA, Australia. He is the author of several books published by multiple major publishers, including Elsevier, Springer, Taylor and Francis, and John Wiley & Sons. He is a member of the Institution of Engineers Australia and a member of the Australian Association for Engineering Education.

Kenji Ikeda has been an associate professor at Tokushima University, Japan, since 1994. He received his BE, ME, and PhD degrees from the University of Tokyo, Japan, in 1986, 1988, and 1991, respectively. His research interests include control engineering and system identification.

Mikio Deguchi is a professor at the National Institute of Technology, Niihama College, Japan. He received his BE, ME, and DrEng degrees from Kyoto University, Japan, in 1983, 1985, and 2001, respectively. From 1985 to 1994, he was employed by the Mitsubishi Electric Corporation and engaged in the development of high-performance manufacturing technology for silicon solar cells. His research interests include semiconductor technology, plasma technology, electronic circuits, and science education.